ISSN 1746-7659, England, UK
Journal of Information and Computing Science
Vol. 6, No. 2, 2011, *pp*. 143-151

Noise Separation from Multiple Copy Images Using the FastICA Algorithm

Hongbo Chen and Zhencheng Chen +

Institute of Biomedical Engineering, Guilin University of Electronic Technology, Guilin, Guangxi, 541004 China

(*Received January 15, 2010, accepted March 20, 2010*)

Abstract. This paper proposes an effective method to separate noise from multiple copy images (MCIs). Suppose that noise and original image are mutually independent in mixed signals, the mixed signals are thus decomposed to an original image independent component and a noise component by using fast independent component analysis (FastICA). The original image independent component is selected to reconstruct the resulting image according to the standard deviation of its time course. By modeling the noise as Gaussian, experimental results show that zero-mean and nonzero-mean Gaussian noises can be separated effectively from multiple copy images by the proposed method, which is effective in the case of stable and unstable noise intensity.

Keywords: multiple copy images, noise separation, the fast independent component analysis (FastICA)

1. Introduction

The rapid development of image acquisition technology has made it possible to acquire multiple copy images (MCIs) in real time. For a degraded video sequence, suppose that a few consecutive frames in which motion is not significant are chosen, and that the registration problem has already been taken into account, the frames can be viewed as multiple noisy copies of the same image. When an unsatisfactory electronic form of the image is obtained by scanning a picture, one can scan the picture repeatedly to get multiple copies, and then remove the noise from the copies employing a denoising algorithm of MCIs to acquire a noise-free image. An increasing number of applications can be found for denoising methods for MCIs [1-5].

The standard method for combining multiple copies is to compute their weighted average. Since the wavelet transform filter is shown to effectively denoise a single noisy image, some researchers applied wavelet transform into noise separation from MCIs. FENG et al. [6] presented a color correction algorithm based on wavelet transform for noisy multiview images to eliminate noise effect to the fullest extent. QIAO et al. [7] introduced a multi-channel wavelet filter bank to recover palm print images with serious deformation. CHANG et al. [8, 9] presented a method that combined two operations for MCI denoising, namely, averaging operation and wavelet thresholding, and discussed the problems of near-optimal thresholds for each ordering of the two operations. In the methods based on wavelet transform, the threshold operation was performed on the coefficients of the detail subbands while thresholding is a nonlinear technique, thus the denoising effect was limited.

In MCIs, the original image signal is still, while the noise signal varies in each image. The source of the original image signal is different from that of the noise signal. Therefore, the noise and the original image can be viewed as mutually independent components, and independent component analysis (ICA) can be used to separate noise from MCIs. In algorithms for ICA, the fast independent component analysis (FastICA) [10] has the advantage of fast convergence. The problem of noise separation in MCIs by FastICA algorithm was studied in this paper. The mixed signals were decomposed using FastICA. Then, the original image independent component (OIIC) was selected to reconstruct the resulting image according to the standard deviation of its time course. By modeling noise as a zero-mean or nonzero-mean *Gaussian* noise in the case of stable and unstable noise intensity, experimental results were presented to show the effectiveness of the proposed method.

+ Corresponding author. Tel.: +86-773-2293135;
E-mail address: hongbochen@163.com.

2. Principle of FastICA

The FastICA algorithm is based on fixed-point algorithm that shares most benefits of neural leaning rules. The main advantage of the fixed-point algorithm is that its convergence is very fast. The ICA problem is formulated as the search for a linear transformation that minimizes the mutual information of the resulting components. This is roughly equivalent to finding directions in which negentropy is maximized; the latter can likewise be considered as projection pursuit directions [10].

In the simplest case, an approximation of negentropy is of the form

$$J(y_i) \approx c[E\{G(y_i)\} - E\{G(v)\}]^2 \tag{1}$$

where $G(\cdot)$ is practically any nonquadratic function, c is an irrelevant constant, and v is a *Gaussian* variable of zero-mean and unit-variance. $E(\cdot)$ is a mathematical expectation. To find an independent component, or a projection pursuit direction as $y_i = w^T x$, the function $J_{G(W)}$ is maximized. The $J_{G(W)}$ is given by

$$J_{G(w)} = [E\{G(w^T x)\} - E\{G(v)\}]^2 \tag{2}$$

where w is an m-dimensional (weight) vector constrained so that $E\{(w^T x)^2\} = 1$. Thus, the problem of ICA can be deduced to the optimization problem

$$\text{maximize} \quad \sum_{i=1}^{n} J_{G(w_i)}, wrt.w_i, i = 1,...,n \tag{3}$$

$$\text{under constraint} \quad E\{(w_k^T x)(w_j^T x)\} = \delta_{jk} \tag{4}$$

where at the maximum, every vector $w_i, i = 1,...,n$ gives one of the rows of the weighted matrix W. The ICA transformation is then given by $Y = WX$, and the signal can be reconstructed by $X = W^{-1}Y$, where X is the synthetical matrix of mixed signals and Y is the synthetical matrix of the ICs.

3. Scheme of noise separation

3.1. FastICA decomposition

In image processing, the ICA method is classified as Temporal ICA (TICA) and Spatial ICA (SICA) according to the formation of the mixed matrix used for decomposition [11,12]. In the SICA method, standard deviation of time course can be used to identify the noise component. The computation time of SICA is less than that of the TICA due to the different formation of the mixed matrix to be decomposed. Therefore, SICA was employed to construct the mixed matrix in the algorithm.

In SICA, every image is reshaped to a row vector, with all row vectors combining into a mixed matrix $X_{n\times(MN)}$, where n is the number of images and M and N are the height and the width of the image, respectively. The matrix X is then decomposed to $Y = WX$ using the FastICA algorithm. All rows in matrix Y are ICs in space. Every column of W^{-1} is the time course of the corresponding ICs.

To validate the ICA approach, an underlying assumption is that, at most, one source in the mixture model can be allowed to be a *Gaussian* source. This is because a linear mixture of *Gaussian* sources is still a *Gaussian* source [13]. Thereby, only two ICs can be obtained from mixed signals because of the *Gaussian* noise. One of the ICs represents the static original image, and another the variable noise.

3.2. Selection of original image IC

Suppose MCIs are degraded by Gaussian noise. Then, based on FastICA, MCIs are decomposed into the two ICs previously mentioned, as shown in Fig. 1.

It is easy to find that there exists an obvious difference between the time courses of the two ICs. For OIIC, the time course varies slightly, which implies that the signal from OIIC is static. Thus, the signal determined by OIIC is the original image. For the noise IC (NIC), the time course varies significantly, which implies that the signal from NIC is variable. Consequently, the signal determined by NIC is the noise. The standard deviation can be used to describe different properties of a stochastic variable. The standard

deviation of the time course of the OIIC is smaller than that of the NIC. Consequently, the standard deviation is used to select the OIIC. Standard deviation is defined as

$$\sigma_i = \sqrt{\sum_{j=1}^{n}(t_{ij} - m_i)^2 / n} \tag{5}$$

where σ_i denotes the standard deviation, t_{ij} the j^{th} value, m_i the mean of the time course of the i^{th} IC, respectively, and n is the dimension of the time course, that is, the number of MCIs.

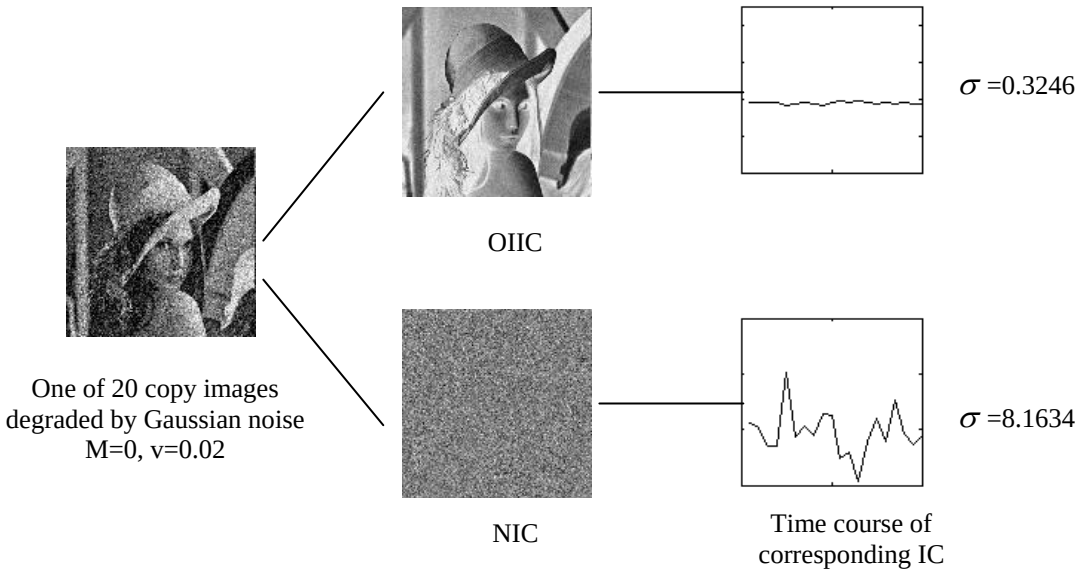

Fig. 1 OIIC and NIC. Two ICs are mapped into a grayscale image using command 'mat2gray' in Matlab

3.3. Algorithm description for noise separation

The architecture of the noise separation based on FastICA is shown in Fig. 2. The process of denoising includes four steps:

Step 1. The mixed matrix is formed according to SICA.

Step 2. The mixed matrix is decomposed using FastICA, and two ICs are obtained.

Step 3. The OIIC is selected according to the standard deviation of time course.

Step 4. The resulting image is reconstructed with the selected IC.

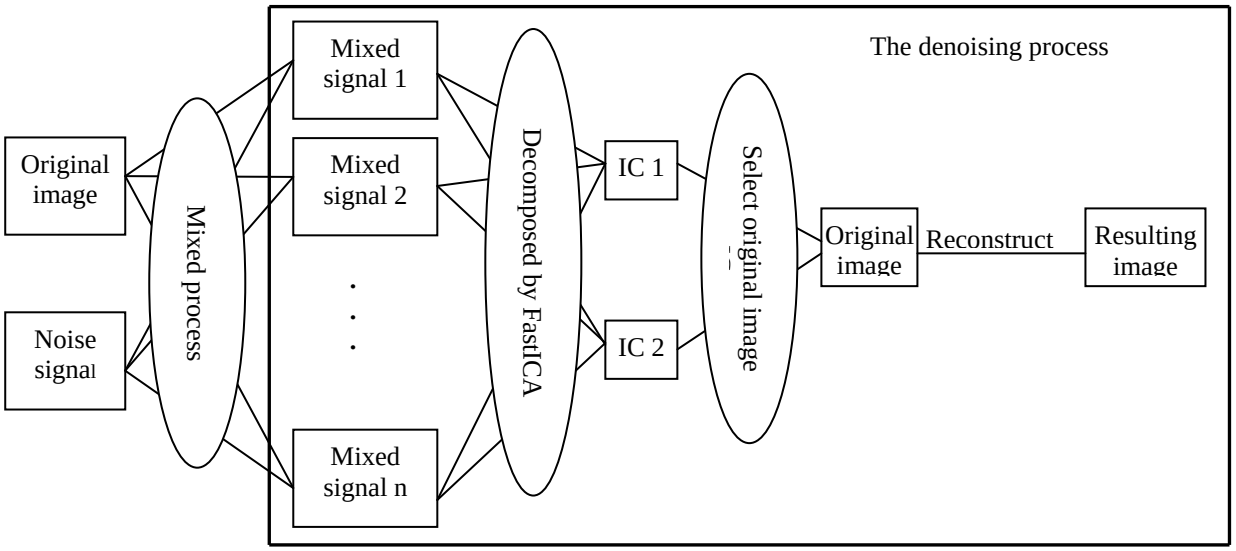

Fig. 2 Process of noise separation in MCIs based on FastICA

4. Experimental results

4.1. Evaluation scheme for denoising results

A 128×128 block grayscale image from *Lena* will be used as the test image in this study. The mean square error (ξ) and Pearson correlation coefficients (ρ) between the resulting image and the original image were employed to evaluate the effect of noise separation. In addition, the Spatial Frequency (τ) [14] was employed to evaluate the visual quality of the resulting image.

The mean square error (ξ) is defined as

$$\xi = \sqrt{\sum_{i=1}^{M}\sum_{j}^{N}[R(i,j)-O(i,j)]^2/(MN)} \tag{6}$$

and the Pearson correlation coefficient (ρ) is defined as

$$\rho = \frac{\sum_{i=1}^{M}\sum_{j=1}^{N}(R(i,j)-\bar{R})(O(i,j)-\bar{O})}{\sqrt{\sum_{i=1}^{M}\sum_{j=1}^{N}(R(i,j)-\bar{R})^2}\sqrt{\sum_{i=1}^{M}\sum_{j=1}^{N}(O(i,j)-\bar{O})^2}} \tag{7}$$

The Spatial Frequency (τ) is defined as

$$\tau = \sqrt{\frac{1}{MN}\left[\sum_{i=1}^{M}\sum_{j=2}^{N}(R(i,j)-R(i,j-1))\right]+\left[\sum_{i=2}^{M}\sum_{j=1}^{N}(R(i,j)-R(i-1,j))\right]} \tag{8}$$

where R is the denoising resulting image, O is the original image, M and N are the height and the width of the image, respectively, and $\bar{R}$ and $\bar{O}$ are the average of R and O, respectively. They are defined as:

$$\bar{R} = \frac{\sum_{i=1}^{M}\sum_{j=1}^{N}R(i,j)}{MN} \tag{9}$$

$$\bar{O} = \frac{\sum_{i=1}^{M}\sum_{j=1}^{N}O(i,j)}{MN} \tag{10}$$

The ξ is a measure of the difference between the resulting image and the original image. If ξ is smaller, it means that the difference is small and the denoising result is better. The ρ is a common measure of the correlation between the resulting image and the original image, and it is not associated with the offset caused by the nonzero-mean noise. The τ indicates the overall activity level in the spatial domain in an image.

To view the effectiveness of the proposed algorithm, the method of average operation and those based on wavelet thresholding technique [8, 9] are adopted for testing. In the methods based on the wavelet thresholding technique, two operations, averaging and thresholding, are combined. According to the order of the two operations, the methods based on wavelet thresholding technique were divided into two algorithms, averaging then thresholding (AT) and thresholding then averaging (TA). Both algorithms are adopted for the test. It is supposed that the pixels in MCIs have one-to-one correspondence and the process of registration of MCIs is not discussed here.

4.2. The case of stable noise intensity

Stable noise intensity means that noise parameters remain invariable in the process of acquiring MCIs, and that noise intensities in MCIs are the same. In this experiment, there are eight groups of experimental results shown in Table 1 and Table 2. In these results, the number of MCIs is set to 14. To demonstrate visual quality, a group of resulting images is shown in Fig. 3.

Table 1 ξ comparison of denoising results in the case of stable noise intensity

	Noise mean	Noise variance	ξ of noisy image	ξ of proposed method	ξ of average operation	ξ of Wavelet (TA)	ξ of Wavelet (AT)
1	0	0.1	67.5844	20.2145	23.6791	20.9929	21.4497
2	0	0.2	84.0872	27.8463	32.1220	27.2406	27.5040
3	0.1	0.1	73.4576	29.3510	34.8160	30.6238	30.9090
4	0.1	0.2	88.9202	31.9460	40.2922	34.7484	34.2765
5	0.2	0.1	82.4768	43.7402	52.0718	49.3254	49.5145
6	0.2	0.2	94.9018	47.4210	53.4420	49.4307	49.0811
7	0.3	0.2	102.4304	53.2389	68.2740	65.3014	65.0765
8	0.3	0.3	108.0776	56.5658	67.2478	63.4304	62.8982

Table 2 ρ comparison of denoising results in the case of stable noise intensity

	Noise mean	Noise variance	ρ of noisy image	ρ of proposed method	ρ of average operation	ρ of Wavelet (TA)	ρ of Wavelet (AT)
1	0	0.1	0.8124	0.8260	0.8169	0.7863	0.7682
2	0	0.2	0.6889	0.7215	0.6915	0.6688	0.6499
3	0.1	0.1	0.8188	0.8475	0.8279	0.7973	0.7783
4	0.1	0.2	0.7021	0.7181	0.7039	0.6823	0.6622
5	0.2	0.1	0.8075	0.8328	0.8138	0.7820	0.7630
6	0.2	0.2	0.6880	0.7116	0.7069	0.6678	0.6480
7	0.3	0.2	0.6483	0.6903	0.6538	0.6317	0.6129
8	0.3	0.3	0.5809	0.6197	0.5849	0.5640	0.5459

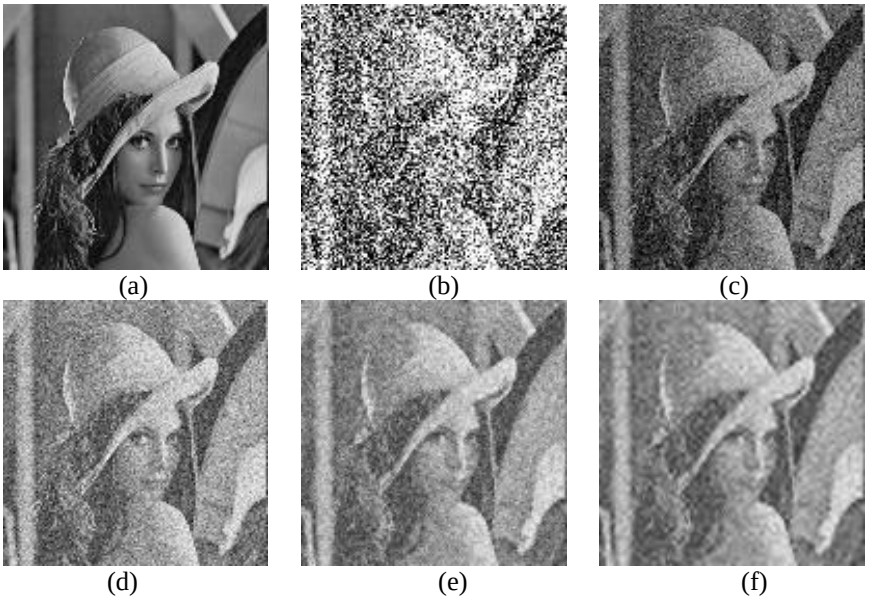

(a) (b) (c)

(d) (e) (f)

Fig. 3 Comparison of the resulting images in the case of stable noise intensity. (a) Original image; (b) One of the 14 noisy images (Mean = 0.2, Variance = 0.2); (c) Resulting image of the proposed method (τ = 56.4062); (d) Resulting image of an average operation (τ = 58.4508); (e) Resulting image of Wavelet (TA) (τ = 34.1049); and (f) Resulting image of Wavelet (AT) (τ = 22.2940).

Table 1 shows that the ξ of the proposed method is much smaller than those of the other methods in the condition of nonzero-mean noise, though it is almost equal to that of average operation in the condition of zero-mean noise. Table 2 shows the ρ of the proposed method is the largest, indicating that the resulting image of the proposed method is most relevant to the original image without taking into account the offset

caused by the nonzero-mean of noise. The ρ of the wavelet-based methods is even smaller than that of the noisy image mainly because thresholding is a nonlinear technique among wavelet-based methods. From Fig. 3, the τ s of the FastICA method is almost equal to that of an average operation and much larger than those of the wavelet-based methods. The visual qualities of the resulting images of the proposed method and the average operation are the best. The detail in this original image can be well preserved. Therefore, the new method is effective for both zero-mean noise and nonzero-mean noise, and the same time, it gets good visual quality.

4.3. The case of unstable noise intensity

Unstable noise intensity means that the noise parameters change in the process of acquiring MCIs. In addition, it means that noise intensities in MCIs are different from each other. There are three possible cases for unstable noise intensity: 1) noise mean is invariable but noise variance varies; 2) noise mean varies, but noise variance maintains stable; and 3) both noise mean and variance are different in each MCI. Tables 3 and 4 show four groups of experimental results for the different cases. A group of resulting images is shown in Fig. 4.

Table 3 ξ comparison of denoising results in the case of unstable noise intensity

Number of MCIs	Noise mean	Noise variance	ξ of proposed method	ξ of average operation	ξ of Wavelet (TA)	ξ of Wavelet (AT)
20	0	from 0.02 to 0.4, increasing by 0.02.	21.7230	24.2832	23.4358	21.8689
20	0.1	from 0.02 to 0.4, increasing by 0.02.	29.2555	35.1936	33.9370	32.8208
20	from 0.01 to 0.2, increasing by 0.01.	0.1	28.3330	31.9752	30.8094	30.2594
20	from 0.01 to 0.2, increasing by 0.01.	from 0.02 to 0.4, increasing by 0.02.	28.5570	34.2124	32.9909	31.8625

Table 4 ρ comparison of denoising results in the case of unstable noise intensity

Number of MCIs	Noise mean	Noise variance	ρ of proposed method	ρ of average operation	ρ of Wavelet (TA)	ρ of Wavelet (AT)
20	0	from 0.02 to 0.4, increasing by 0.02.	0.8278	0.6869	0.6992	0.6846
20	0.1	from 0.02 to 0.4, increasing by 0.02.	0.8331	0.7203	0.7095	0.6948
20	from 0.01 to 0.2, increasing by 0.01.	0.1	0.8610	0.8299	0.8170	0.8016
20	from 0.01 to 0.2, increasing by 0.01.	from 0.02 to 0.4, increasing by 0.02.	0.8198	0.7188	0.7082	0.6936

When the noise mean is zero and noise variance varies, the ξ of the four methods are almost the same and all methods are effective in terms of the mean square error and Pearson correlation coefficients. The ξ of the proposed method is smaller than those of the other methods when the noise mean varies, while the ρ of the proposed method is larger than those of the other methods. Therefore, the resulting image of the proposed method is closer to the original image than that of the other methods. Fig. 4 shows that the τ s of the FastICA method is almost equal to that of the average operation and much larger than those of the

wavelet-based methods. Details in the original image are likewise well preserved in the resulting images of the FastICA method and the average operation, images that are the best of the lot. As shown above, the proposed algorithm is more effective than other methods for the case of unstable noise intensity.

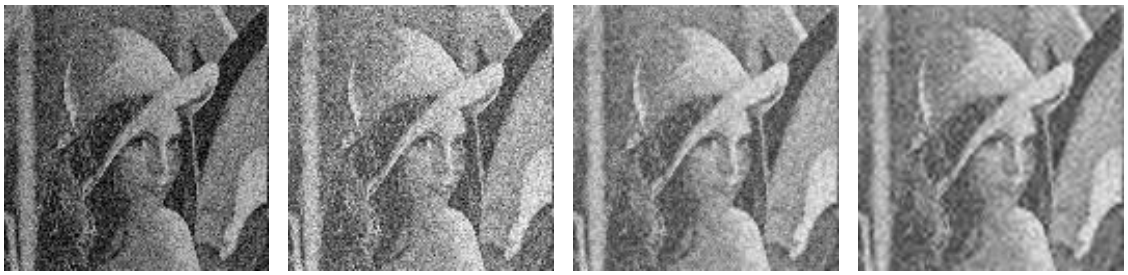

(a) (b) (c) (d)

Fig. 4 Comparison of the resulting images in the case of unstable noise intensity. (Mean = 0.1, Variance varies from 0.02 to 0.4 increasing by 0.02); (a) Resulting image of the proposed method (τ = 47.5566); (d) Resulting image of average operation (τ = 49.8862); (e) Resulting image of Wavelet (TA) (τ = 37.9167); and (f) Resulting image of Wavelet (AT) (τ = 26.6179)

5. Discussions

5.1. The number of requisite copy images

In this experiment, four cases of *Gaussian* noise were considered. The influence of the number of MCIs on the denoising results is shown in Fig. 5. In the figure, it is seen that:

1) When the number of MCIs increase, the ξ of the resulting image becomes smaller, that is, the effect of denoising gets better. Theoretically, the noise in the image can be entirely removed when the number of MCIs is infinite.

2) When the number of MCIs is more than 14, the ξ of the resulting image decreases slightly as the number of MCIs increase.

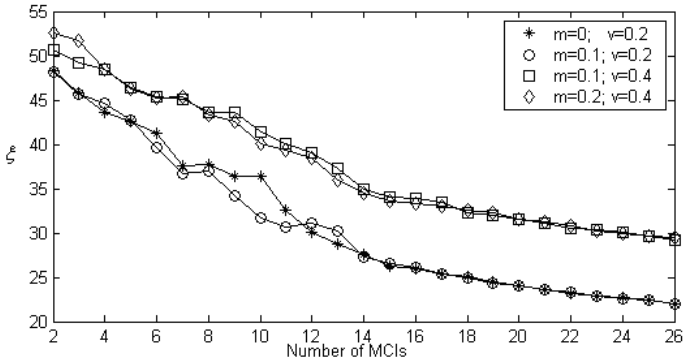

Fig. 5 Influence of the number of MCIs upon the denoising result.

5.2. The influence of noise intensity on denoising results

The denoising result is different from the different noise intensity. The influence of the noise variance on the denoising result is shown in Fig. 6. When the noise mean is 0.1 and the noise variance varies from 0.04 to 0.8, the ξ of the resulting image becomes greater with the increment of the noise variance. Thus, the visual quality of the resulting images becomes poor.

The influence of the noise mean on the denoising result is shown in Fig. 7. While noise variance is 0.2 and noise mean varies from 0.02 to 0.4, the ξ s of the resulting images are almost equal to the different noise means. It implies that noise mean has little influence on the denoising result.

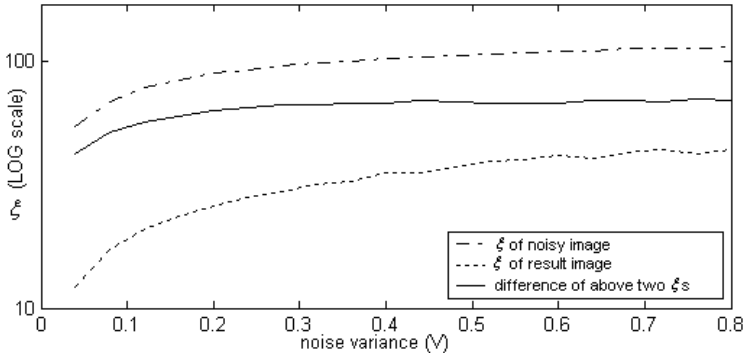

Fig. 6 Influence of the noise variance upon the denoising result with the noise mean M = 0.1; the number of MCIs is set to 14.

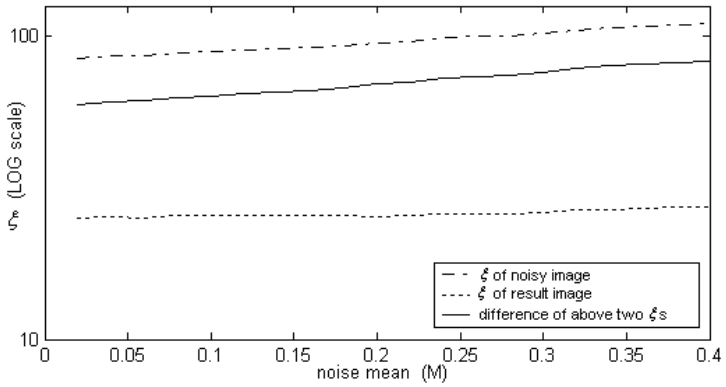

Fig. 7 Influence of the noise mean upon the denoising result with the noise variance V = 0.2; the number of MCIs is set to 14.

6. Conclusions

1) An effective denoising method was proposed for MCIs based on FastICA. The mixed matrix was formed as a SICA. Suppose noise and original image are mutually independent and the noise was modeled as *Gaussian*, then NIC and OIIC are obtained from mixed signals based on FastICA. The original image IC, with which the resulting image could be reconstructed, was selected according to the standard deviation of the time course of corresponding IC.

2) Experimental results show that the proposed method is effective for both the zero-mean and nonzero-mean *Gaussian* noise. The best effectiveness for noise separation can be obtained in cases of stable and unstable noise intensity. In addition, details in the original image can be well preserved in the resulting images.

3) The proposed algorithm can be used as a means for noise separation in remote sensing images, medical images, and image sequences.

7. References

[1] C. Quan, X. Kang, and C.J.Tay. Speckle noise reduction in digital holography by multiple holograms. *Optical engineering*. 2007, **46** (11): 115801-1-115801-6.

[2] Bruno, M., Jovan, G.B., and Miles, N.W. Noise and sampling analysis for multiple-image radiography. *3rd IEEE International Symposium on Biomedical Imaging (ISBI'06), Arlington WA USA: 2006IEEE*. 2006, 3, pp. 1232-1235.

[3] Boecker, D., Zybin, A., Niemax, K., Grunwald, C., and Mirsky, V.M. Noise reduction by multiple referencing in surface plasmon resonance imaging. *Review of Scientific Instruments*. 2008, **79** (2part1): 23110-1-23110-6

[4] Liu, R.H., and Li, F. Robust remove noise using multiple degraded images. *Chinese Journal of Electrinocs*. 2008, **17** (2): 305-308

[5] Atsushi, Y., Masayuki, K., and Toru, K. Removal of adherent noise in images by using multiple cameras. *Electrical Engineering in Japan*. 2008, **164** (3): 50-59.

[6] Feng, S., Jiang, G., Yu, M., and Chen, K. A color correction algorithm for noisy multi-view images. *Chinese*

Optics Letters. 2007, **5** (1): 28-30.

[7] Qiao, Y.H., Li, F.Q., Qiao, A.K., Zhang, J.H., Liang, K., and Zeng, Y.J. Palm print image recovery and de-noising via multi-channel wavelet filter bank. *Journal of Medical Engineering & Technology*. 2006, **30**(5): 310-314.

[8] Chang, S.G., Yu, B., and Vetterli, M. Wavelet thresholding for multiple noisy image copies. *IEEE Trans. on Image Processing.* 2000, **9** (9): 1631-1635.

[9] Chang, S.G., Yu, B., and Vetterli M. Multiple copy image denoising via wavelet thresholding. *IEEE Int. Conf. on Image Processing*. 1998, pp. 545-549

[10] Hyvarinen, A. Fast and robust fixed-point algorithms for independent component analysis. *IEEE Trans. on Neural Networks.*1999, **10** (3): 626-634

[11] Wang, P.S., Wu Y.T., Hung, C.I., Kwan, S.Y., Teng, S., and Soong, B.W. Early detection of periodic sharp wave complexes on EEG by independent component analysis in patients with Creutzfeldt-Jakob disease. *Journal of Clinical Neurophysiology*. 2008, **25** (1): 25-31

[12] Reidl, J., Starke, J., Omer, B.D., Grinvald, A., and Spors, H. Independent component analysis of high-resolution imaging data identifies distinct functional domains. *NeuroImage.* 2007, **34** (1): 94-108.

[13] Wang, J., and Chang, C.I. Independent component analysis-based dimensionality reduction with applications in hyperspectral image analysis. *IEEE Trans. on Geoscience and Remote Sensing*. 2006, **44** (6): 1586-1600.

[14] Ahmet, M.E. and Paul S.F. Image quality measures and their performance. *IEEE Transactions on Communications.* 1995, **43**(12): 2959-2965.